Final Draft
of the original manuscript:

Bieser, J.; Aulinger, A.; Matthias, V.; Quante, M.; Denier van der Gon, H.A.C.:
Vertical emission profiles for Europe based on plume rise calculations
In: Environmental Pollution (2011) Elsevier

DOI: 10.1016/j.envpol.2011.04.030

Vertical emission profiles for Europe based on plume rise calculations

J. Bieser [a,b,*], A. Aulinger [a], V. Matthias [a], M. Quante [a,b], H.A.C. Denier van der Gon [c]

[a] Helmholtz Zentrum Geesthacht, Institute of Coastal Research, D-21502 Geesthacht, Germany

[b] Leuphana University Lüneburg, Institute of Environmental Chemistry, D- 21335 Lüneburg, Germany

[c] TNO, Netherlands Organisation for Applied Scientific Research, P.O.Box NL-80015, Utrecht, The Netherlands

Article info

Article history:

Received 17 Dec 2010
Revised 12 Apr 2011
Accepted 17 Apr 2011

Key words:

Vertical distribution
Emission height
Point source
Vertical emission profiles

Abstract

The vertical allocation of emissions has a major impact on results of Chemistry Transport Models. However, in Europe it is still common to use fixed vertical profiles based on rough estimates to determine the emission height of point sources. This publication introduces a set of new vertical profiles for the use in chemistry transport modeling that were created from hourly gridded emissions calculated by the SMOKE for Europe emission model. SMOKE uses plume rise calculations to determine effective emission heights. Out of more than 40 000 different vertical emission profiles 73 have been chosen by means of hierarchical cluster analysis. These profiles show large differences to those currently used in many emission models. Emissions from combustion processes are released in much lower altitudes while those from production processes are allocated to higher altitudes. The profiles have a high temporal and spatial variability which is not represented by currently used profiles.

1. Introduction

Anthropogenic emissions for Chemistry Transport Models (CTMs) are usually created by 'down-scaling' of national emissions on a grid using source sector specific proxies. This means that aggregated annual total emissions provided by official reports or expert estimates are disseminated spatially and temporally over the model domain. The emissions can be allocated to three different source types: area, line and point sources. Area and line sources are disaggregated using spatial surrogates, e.g. population density, land use, transportation networks. For point sources that are usually large industrial plants with tall stacks the exact geographical location is known. While spacial surrogates are used to disaggregate area and line sources the disaggregation of point sources requires information like stack height or exit velocity and meteorological data because point source emissions are subject to plume rise effects. The altitude point source emissions are allocated to is called the effective emission height. It is defined as the altitude where momentum and buoyancy of an emitted plume dissipate and do no longer drive the rise of the plume. Depending on the meteorological conditions the effective emission height can be higher, equal, or sometimes even lower than the stack height of the source.

However, most emission models used in Europe do not include explicit plume rise algorithms and use fixed vertical profiles instead (Benedictow, 2009; Schaap et al., 2005; Visschedijk and Denier van der Gon, 2005; Visschedijk et al., 2007) that describe the emissions in

Correspondence to: Johannes Bieser
email: johannes.bieser@hzg.de
phone: +49 4152 87 2334
fax: +49 4152 87 2332
address: Helmholtz-Zentrum Geeshacht
Max-Planck-str. 1
D-21502 Geesthacht; Germany

different model layers as fractions of the total emissions in a column of the model domain. The vertical profiles used up to date are rough estimates based on coarse source categories and have a low vertical resolution. Also, comparing different sets of profiles reveals large differences in the estimated effective emission heights. Most European air quality studies and intercomparisons use the vertical distributions of the European Monitoring and Evaluation Program (EMEP) model (Vidic, 2002). These profiles are based on five years of plume rise calculations for the city of Zagreb, Croatia, and may not be representative for other European regions. Further, the coarse vertical resolution of 6 layers between 92m and 1100m does not match the resolutions typically used for regional CTMs which have 20-40 vertical layers with near surface layer heights between 20m and 60m. A large fraction of the emissions is allocated to altitudes above 500m. Since the profiles are annual averages they do not consider the diurnal and seasonal cycles. Because the planetary boundary layer (PBL) height differs strongly between night and day as well as between summer and winter, annual average profiles are likely to under- or overpredict the amount of emissions above the PBL. The meteorological data was taken from radio soundings over Zagreb, gas temperature and exit velocity were estimated depending on stack height. The EMEP profiles distinguish six source categories, based on the Selected Nomenclature of sources of Air Pollution (SNAP) (Table1). SNAP is a standard defined by the CORINAIR guidebooks which ensures that emissions reported by different nations are comparable (European Environmental Agency, 2007). De Meij et. al (2006) used a modified version of the EMEP profiles with the global CTM TM5 (Krol et al., 2005). They contain separate effective emission heights for gaseous and aerosol species but only distinguish four vertical layers. Although these profiles are based on the EMEP profiles a comparison of the two datasets revealed large differences.

Profiles of effective emission heights received little attention in the modeling community. However, the altitude point source emissions are released into the atmosphere are of major importance for CTM calculations. As Figure 1 and 2 indicate, a large share of anthropogenic emissions into the atmosphere is emitted by point sources. The dominant species emitted by point sources are Sulfur oxides (SO_X) (Fig. 1) followed by carbon monoxide (CO), nitrogen oxides (NO_X), and particulate matter (PM). The vertical distribution of these emissions has a large effect on the concentrations calculated by CTMs (De Meij, 2006; Pozzer, 2009), because it influences the chemical composition of air and removal and transport of substances. As an example, the formation of secondary pollutants like ozone is affected because first and higher order chemical reaction rates depend on the

Table 1

Description of SNAP sectors and their implementation in the SMOKE-EU emission model. (SNAP sector 2 is considered an area source in the SMOKE-EU emission model. Still EMEP uses vertical profiles for this source sector)

Sector	Emission type	Description
SNAP 1	point source	Combustion in energy and transformation industries
SNAP 2	area source	Non-industrial combustion plants
SNAP 3	point source	Combustion in manufacturing industry
SNAP 4	point source	Production processes
SNAP 5	point source	Extraction of fossil fuels
SNAP 6	area source	Solvent use and other product use
SNAP 7	line source	Road transport
SNAP 8	line source	Other mobile sources and machinery
SNAP 9	point source	Waste treatment and disposal
SNAP 10	area	Agriculture

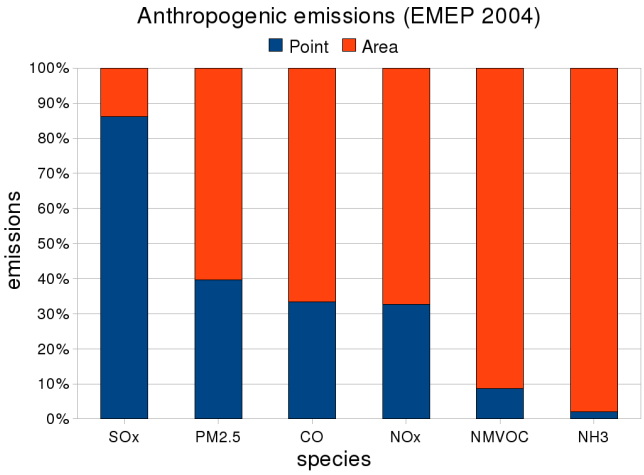

Figure 1: Relative amount of point-source emissions compared to total emissions depending on species. (http://www.ceip.at/emission-data-webdab/emissions-used-in-emep-models/)

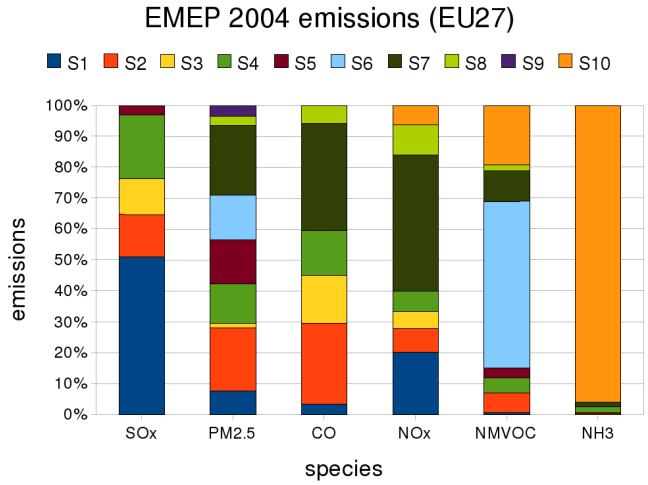

Figure 2: Annual emissions from different SNAP sectors. More than 80% of all point source emissions are allocated to the SNAP sectors 1, 3, and 4. Roughly half of the NMVOC emission from point-sources is related to SNAP sector 5.

concentrations of the reactants that can be different in each model layer. One of the most important output data of air quality models are ground level concentrations. A reduction of NO_X emissions for example leads to higher ozone concentrations due to less ozone degradation at night (Wickert 2001; Wickert et. al, 2001). The formation of secondary aerosols like ammonium sulfate ($[NH_4]_2SO_4$) and ammonium nitrate (NH_4NO_3) is influenced by the emission height of SO_2. SO_2 is oxidized via photochemistry and in-cloud oxidation to Sulfate (SO_4^{2-}) which then forms ammonium sulfate particles. This process is mostly limited by the available amount of Ammonia (NH_3). Because in the CTM the reaction of ammonium (NH_4^+) with SO_4^{2-} is preferential to the reaction with Nitrate (NO_3^-) ammonium nitrate formation only takes place if no more SO_4^{2-} is available. If less SO_2 is emitted in the near surface layer the formation of ammonium nitrate (NH_4NO_3) aerosols will increase and the concentration of Nitric acid (HNO_3) decrease because more NH_3 is available. The vertical distribution of SO_2 also influences the SO_2 to SO_4^{2-} ratio. Bieser et al. (2011) showed that emitting all SO_2 and primary SO_4^{2-} in the surface layer leads to an annual average increase of SO_2 of 12% and a 4% decrease of SO_4^{2-} concentration in the surface layer compared to CTM results using the EMEP vertical profiles. Besides this, pollutants emitted in the surface layer are much faster removed from the atmosphere by dry deposition than those emitted at higher altitudes. On the other hand all species emitted above the PBL have a much higher atmospheric residence time and are more likely subject to different chemical reactions (e.g. aqueous chemistry in clouds, photolytic reactions) and long-range transport.

The aim of this study is to provide improved vertical emission profiles for the use in emission models that calculate emissions for CTMs like CAMx (Morris et al., 2001), CHIMERE (Vautard et al., 2007), CMAQ (Byun and Ching, 1999; Byun and Schere, 2006), COSMO-ART (Vogel et al, 2009), COSMO-MUSCAT (Wolke et al., 2004), or WRF-CHEM (Grell et al., 2005). The profiles presented here have a vertical resolution which matches the resolution typically used for regional CTMs. The effective emission heights are calculated from official European emission inventories using real world stack information and hourly meteorological fields. In addition, the uncertainties of the profiles connected with model resolution or introduced by uncertainties in stack data and meteorological fields are estimated. Average emission profiles were derived by averaging hourly profiles within different sections of a domain covering Europe with a 54x54km² grid cell size. This procedure yielded emission profiles distinguished by source sector, countries, climate region, season, day and night, and six species. Finally, the total amount of profiles was reduced by merging similar profiles into groups found by means of hierarchical cluster analyses.

2. Methodology

2.1 Preparation of point source emission data

Annual emissions are taken from official European reports and are disaggregated to hourly values for the timespan 1997 to 2006 using the emission model SMOKE-EU (Bieser et al., 2011). SMOKE-EU is an European adaptation of the SMOKE model, the official emission model of the Unites States Environmental Protection Agency (US EPA) (UNC Carolina Environmental Program, 2005).

In the European Union the emissions of major point sources have to be reported periodically since 2001 (EC, 2000). These are merged into a single database called EPER that is supposed to contain all major point sources, i.e. 80% and 90% of all point sources. EPER is available for the years 2001 and 2004. The 2007 report is called 'Pollutant Release and Transfer Register' (PRTR) which is the new, enhanced version of EPER (EC, 2006). For our study we used the data set for 2004 that appeared to be the best evaluated one at that time. In contrast to the EMEP data base EPER and PRTR also contain the exact geographical location as well as a detailed description of the source types using the “Nomenclature statistique des activités économiques dans la Communauté Européenne” (NACE). Because EPER does not include all point sources (among other reasons not all facilities are obliged to report) the emissions from the European Monitoring and Evaluation Program (EMEP) were used to complete the source emissions inventory for this study. In order to merge EPER and EMEP, the EPER source categories needed to be converted to match the reporting structure of EMEP specified by the SNAP system. Point sources only covered by the EMEP data base were spatially disaggregated by means of SMOKE-EU using the CORINAIR land cover dataset (CLC2000). The SNAP sectors 1,3, and 4 are disaggregated using the land cover class 'commercial and industrial units', SNAP5 using 'ports', and SNAP 9 using 'dump sites' as proxy. A detailed description of these procedures including proxies used for other source types can be found in Bieser et al. (2011).

2.2 Calculation of effective emission heights

Within the SNAP nomenclature there are five emission sectors for which vertical emission profiles are relevant (Table 1). Depending on the emission source type typical stack characteristics were attributed to each point-source. The stack properties together with reconstructed hourly meteorological fields are then used for the plume rise calculations with SMOKE-EU to find the effective emission heights for each source in each grid cell and at each hour. Since neither EPER nor PRTR contain data about stack heights, stack size, temperature or exit velocity of the flue these data bases are not directly suitable for plume rise calculations. Therefore we used typical stack characteristics recently published by Pregger and Friedrich (2009). They developed 34 categorized stacks which represent average values of stack height, flue gas temperature, flue gas velocity, and flue gas flow rate derived from 12 699 individual industrial plants from 10 German federal states. The published stack characteristics include arithmetic mean, median and emission-weighted averages for each source type. Pregger and Friedrich calculated effective emission heights for each source type based on equations of the Association of German Engineers (VDI, 1985) which are mainly based on Briggs (1971) using a standard atmosphere (wind speed 4m/s, neutral temperature stratification).

Though the typical stack characteristics provided by Friedrich and Pregger were only derived from stacks in Germany they reflect a large variability of stack properties. For this reason we are confident that our assumption that these stack categories are applicable to all stacks within Europe is well justified. In addition to these the characteristics of a stack for coke ovens by Yang et. al (1998) have been implemented because this source type is not explicitly included in the 34 stack categories of Pregger and Friedrich. The finally 35 different stack characteristics were applied to the EPER sources that are described by the NACE code and then converted to SNAP sectors. The effective emission heights for different SNAP sectors were calculated using SMOKE-EU with 30 vertical layers up to 50 hPa. The model domain covered the entire European continent as shown in Figure 3.

SMOKE-EU includes, like the original SMOKE, plume rise calculations based on the algorithms used in the Regional Acid Deposition Model (RADM)

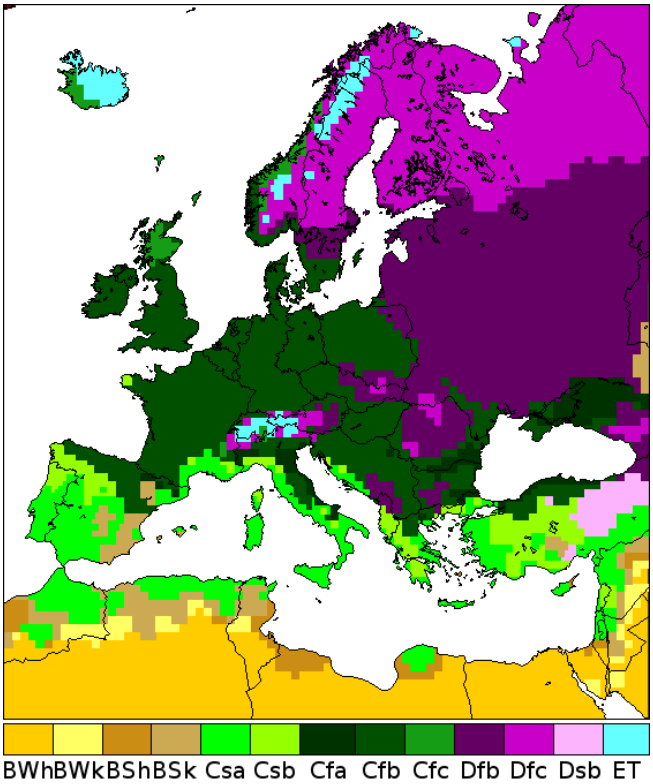

Figure 3: Model domain used in the emission model. Also depicted is a interpolated map of Köppen-Geiger climate classifications for 1976-2000 (based on Rubel and Kottek, 2010). A list of all regions included can be found in Appendix A.

(Byun and Binkowski, 1991; Turner, 1985). RADM uses a layer-by-layer plume penetration and plume rise concept for calculating buoyant plume rise following an approach by Briggs (1969, 1975, 1984). The resulting set of equations as described by Houyoux (1998) is provided in Appendix A. In this approach the 'surface heat flux scale' (Eq. A1) and the 'buoyancy flux' (Eq. A2) are used to calculate an initial plume rise. The formula used for the initial plume rise depends on the stability regime (stable, neutral, unstable) at the stack top (Eq. A3-A6). In addition to the buoyant plume rise SMOKE also considers momentum plume rise (Eq. A7). SMOKE takes further into consideration the mixing height as diagnosed by the meteorological model to determine whether the plume is able to penetrate the PBL top. In total SMOKE distinguishes six different plume rise cases. The equations used to determine the plume rise for each case are shown in supplementary C, Table S3. If the plume penetrates the top of a model layer, the additional plume rise in the next layer is calculated using Equations A8-A11. The total plume rise Δh calculated this way represents the center of the plume when the plume reaches thermodynamic equilibrium with the ambient air. The plume thickness is assumed to be equal to the plume rise. Plume top and plume bottom are calculated following Equations A12 and A13. Finally, the total emissions of a point source are fractionally distributed to the emission layers.

2.3 Uncertainty analyses

The assumptions and methods as well as the input parameters required for the plume rise calculations and the determination of the effective emission heights, respectively, bear several sources of error that introduce a certain amount of uncertainty into the vertical emission profiles. The level of understanding on the physical processes of buoyancy and plume rise as well as on the exhaust mechanisms, at least for major point sources, is relatively high (Emery et al., 2010). Uncertainties connected with the spatial and temporal distribution of the EMEP and EPER emissions was assumed to be of minor relevance. Thus, in order to estimate the level of uncertainty of the here presented profiles frequent plume rise calculations by varying stack characteristics, meteorological fields and the grid resolution of the meteorological model were carried out. The resulting variations of the derived vertical emission profiles were then considered as a measure of uncertainty for the profiles.

2.3.1 Stack characteristics

One part of the uncertainty was considered to be caused by averaging the stack characteristics over many different sources as well as through the application of German stack data to point sources in other European countries. Although the underlying data of the averaged stack characteristics are not known it can be assumed that stack profiles in general follow a similar pattern: For any point source type there are many small plants with low emissions and low stacks and few large plants with high emissions and high stacks. Even when using emission-weighted average profiles the emission heights of the largest sources are probably still underestimated. To take into account a possible underestimation of the major

industrial sources two model runs were carried out where both stack height and exit velocity was increased by 25% and 50%, respectively. On the other hand, higher stacks usually lead to lower exit temperatures. Since the exit temperatures were not changed, however, the effective emission heights might also have been overestimated.

2.3.2 Variability of the meteorological fields

The meteorological variables used to determine the effective emission heights in the plume rise calculations are temperature, pressure, wind speed, water vapor mixing ration and PBL height. To investigate the influence of the inter-annual variability of the meteorology effective emission heights were determined for the 10 years between 1997-2006 using meteorological fields calculated with the COSMO-CLM climate model, a state-of-the-art mesoscale meteorological model (Rockel et al., 2008; Rockel and Geyer, 2008). The COSMO-CLM meteorological fields were calculated using spectral nudging to NCEP reanalysis.

Variability or errors within the meteorological variables are also dependent on the meteorological model and the reanalysis data used for developing the meteorological fields. To take this into account meteorological fields for the years 2000 and 2001 were calculated with COSMO-CLM as well as with the mesoscale meteorological model MM5 (Grell et al., 1995, Matthias et al., 2009). The MM5 model was driven by ERA40 reanalysis data using FDDA as nudging method (Stauffer and Seaman, 1990). This yielded two sets of vertical profiles comprising two years.

2.3.3 Model resolution

To assess the impact of model resolution on the effective emission heights SMOKE-EU runs using COSMO-CLM data on a domain with 72x72km² and a 24x24km² grid cell size were compared to the vertical profiles from the 54x54km² run.

2.4 Generation of vertical profiles

Performing all the different model runs with an output time step of 1 h for 7 290 grid cells (54x54km^2) resulted in a large amount of single vertical profiles that have in a first step been averaged over SNAP sector (Table 1), country, climate region, season and day-time for every chemical species of interest. The set of average profiles comprised 44 976 profiles divided into:

- 5 SNAP sectors (S1, S3, S4, S5, S9)
- 48 countries or political regions subdivided into 13 climate regions
- 4 seasons of the year (Winter, Spring, Summer, Autumn)
- day (6h – 18h UTC) and night (18h – 6h UTC)
- 6 chemical species (SO_2, CO, NO_X, NH_3, PM, NMVOC)

The 48 countries or political regions (see also supplementary A, List S2) were split into climate regions according to the Köppen-Geiger classification (Fig. 3) (Rubel and Kottek, 2010). Table 2 comprises the 13 different climate classes used for spatial aggregation. In cases where a climate region made up more than 95% of the country area exclusively this particular climate region was considered in that country.

Table 2

Köppen-Geiger climate classifications used for spatial aggregation of vertical emission profiles (Fig. 3). A list with all relevant climate classifications for each country can be found in supplementary A, List S2.

Name	Main climate	Precipitation	Temperature
BWh	arid	desert	hot arid
BWk	arid	desert	cold arid
BSh	arid	steppe	hot arid
BSk	arid	steppe	cold arid
Csa	warm temperate	summer dry	hot summer
Csb	warm temperate	summer dry	warm summer
Cfa	warm temperate	fully humid	hot summer
Cfb	warm temperate	fully humid	warm summer
Cfc	warm temperate	fully humid	cool summer
Dfb	snow	fully humid	warm summer
Dfc	snow	fully humid	continental
Dsb	snow	summer dry	warm summer
ET	polar	-	tundra

Further aggregation of similar vertical profiles was achieved by carrying out a hierarchical cluster analysis for each of the five SNAP sectors separately. The method chosen was the cluster analysis according to *Ward* using the squared Euclidean distance as dissimilarity measure (Kaufmann and Rousseeuw, 1990). The distance which separated the groups of similar profiles from each other was determined at that particular aggregation step where the distance between clusters increased by more than 150% relative to the previous aggregation step. This resulted in **73** profile groups. Finally, the mean profile of each cluster group was taken as the representative profile of the group. A list that links each combination of climate region, country, season, time of day, species, and source sector to one of the **73** clustered vertical emission profiles together with a detailed analysis of the profiles can be found in the supplementary material.

3. Results and Discussion

In this chapter a systematic comparison of various emission profiles and groups of emission profiles is given. The values used to compare these profiles are the median altitude, the upper and lower threshold altitudes, the emission range, as well as the maximum and minimum altitudes (Fig. 4). The median altitude is defined as the altitude below which 50% of the emissions occur. The emission range is defined as the region in which two thirds of the emissions take place, 1/3 below and 1/3 above the median altitude. The upper and lower threshold altitudes are the upper and lower borders of the emission range. Thus, 1/6 of the emissions are below the lower and 1/6 are above the upper threshold altitude. The maximum and minimum are the altitudes below, respectively above, which 99% of the emission take place. Figure 4 illustrates an example of these statistical measures. For groups of emission profiles (e.g. all profiles for one SNAP sector, all profiles for a season) the mean and the standard deviation of the median altitudes and the threshold altitudes are used.

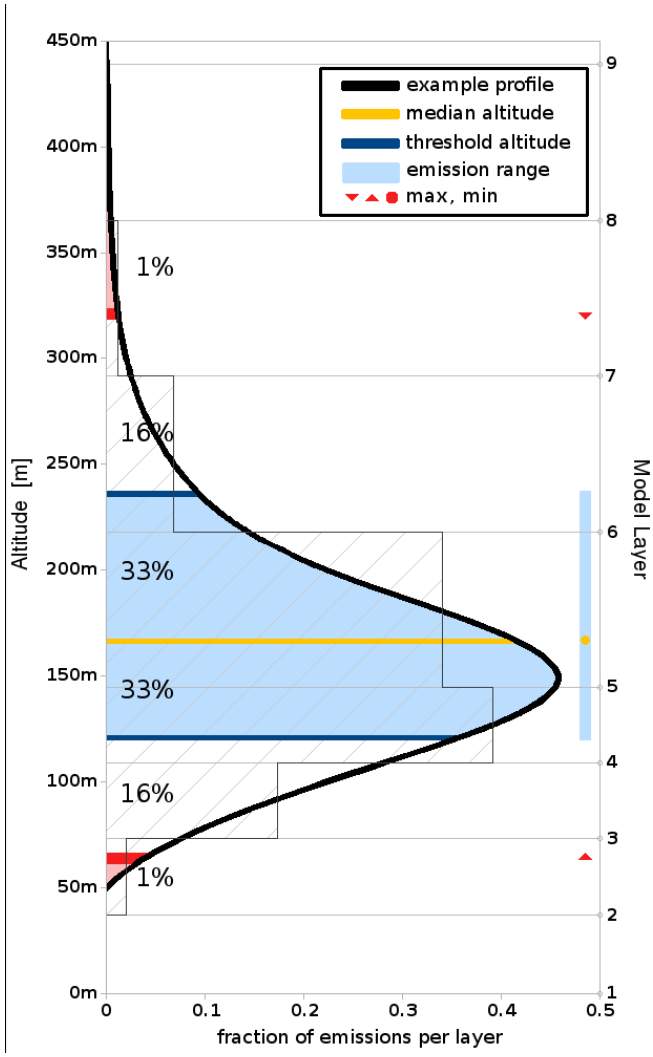

Figure 4: The figure illustrates an example of a vertical emission profiles. The statistical measures used to describe emission profiles in this study are introduced. The median altitude is defined as the altitude below which 50% of the emissions occur. The emission range is defined as the region in which two thirds of the emissions take place, 1/3 below and 1/3 above the mean altitude. The upper and lower threshold altitudes are the upper and lower borders of the emission range. The minimum and maximum are the altitudes below which 1% and 99% of the emissions are emitted.

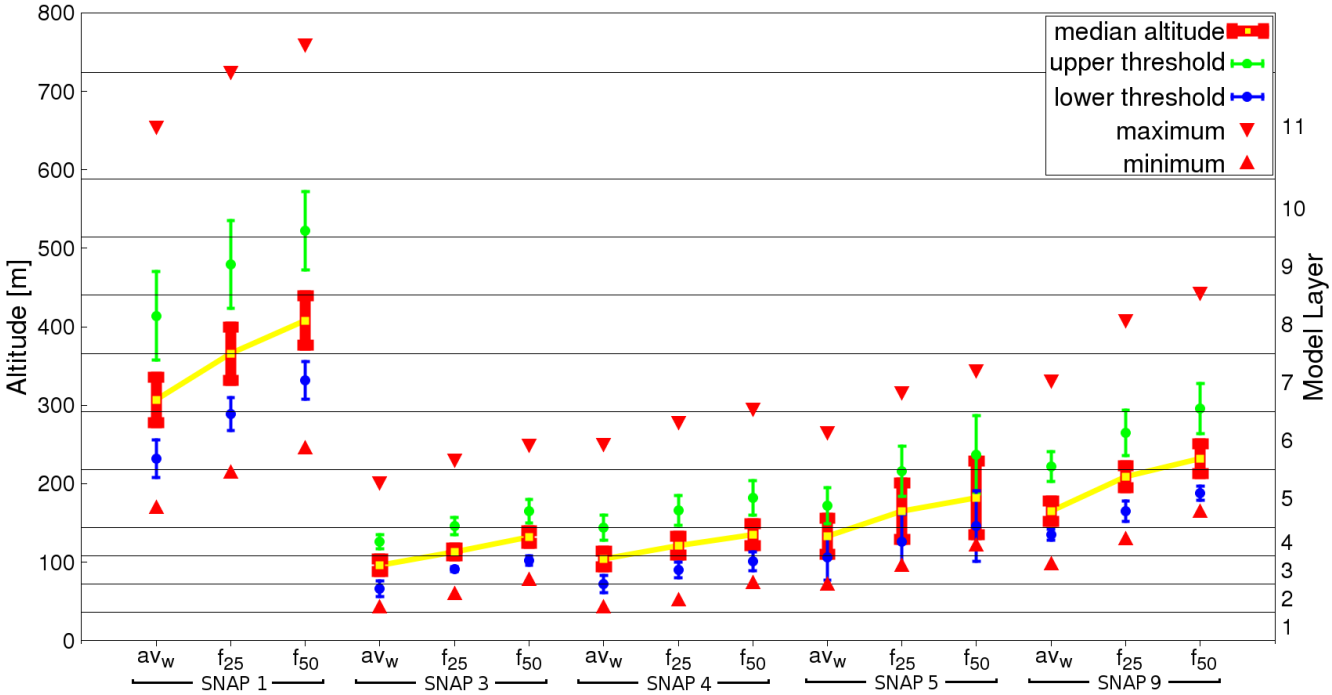

Figure 5: Characterization of emission profiles calculated using different stack properties. For the standard profiles the emission weighted average stack profiles from Pregger and Friedrich (2009) have been used (avw). The values for stack height and exit velocity were increased by 25% (f25) and 50% (f50). It can be seen that for most SNAP sectors the increase is almost linear.

3.1 Evaluation of uncertainties

For the estimation of the influence of stack properties, the meteorological fields, the meteorological models, and the model resolution on effective emission heights aggregated emission profiles for each SNAP sector were compared. This means that the 44 976 spatially and temporally aggregated emission profiles were combined into five groups, one for each SNAP sector. The highest uncertainties were found when using alternative stack characteristics. The lowest uncertainties are due to the model resolution.

We performed two alternative SMOKE-EU runs in order to better understand the uncertainties introduced by stack properties, i.e. (1) +50% case, stack heights and exit velocity increased by 50% and (2) +25% case, stack heights and exit velocity increased by 25%. Results from the +25% and +50% cases were compared to emission profiles calculated using the emission-weighted average stack profiles (default run). The differences between the alternative runs and the default run were analysed for each of the five SNAP sectors containing point sources. The +25% case leads to a 15% to 20% higher average median altitude and a 10% to 20% larger average emission range. The 50% case leads to a 25% to 30% higher average median altitude and a 10% to 20% larger average emission range (Fig. 5). It can be seen that the increase in effective emission height is almost linear with the increase of stack height and exit velocity.

The effect of the inter-annual meteorological variability as simulated with COSMO-CLM for ten consecutive years is small (1-2%). In figure 6 the results for SNAP sector 1 are shown as an example. Comparison of temperature, pressure, wind speed, and water vapour mixing ratio for the different years showed variations which have no relevant influence on effective emission heights (Fig. S13). Of these four meteorological values wind speed has the largest influence on the plume rise calculations (Eq. A4-A7). Also the temperature gradient is important because it is used to determine the atmospheric stability (Eq. A3), while the absolute temperature has only a small effect (Eq. A2). Larger differences were found only for wind speeds above an altitude of 300m. The results of the study on the influence of meteorological parameters are depicted in the supplementary material B.

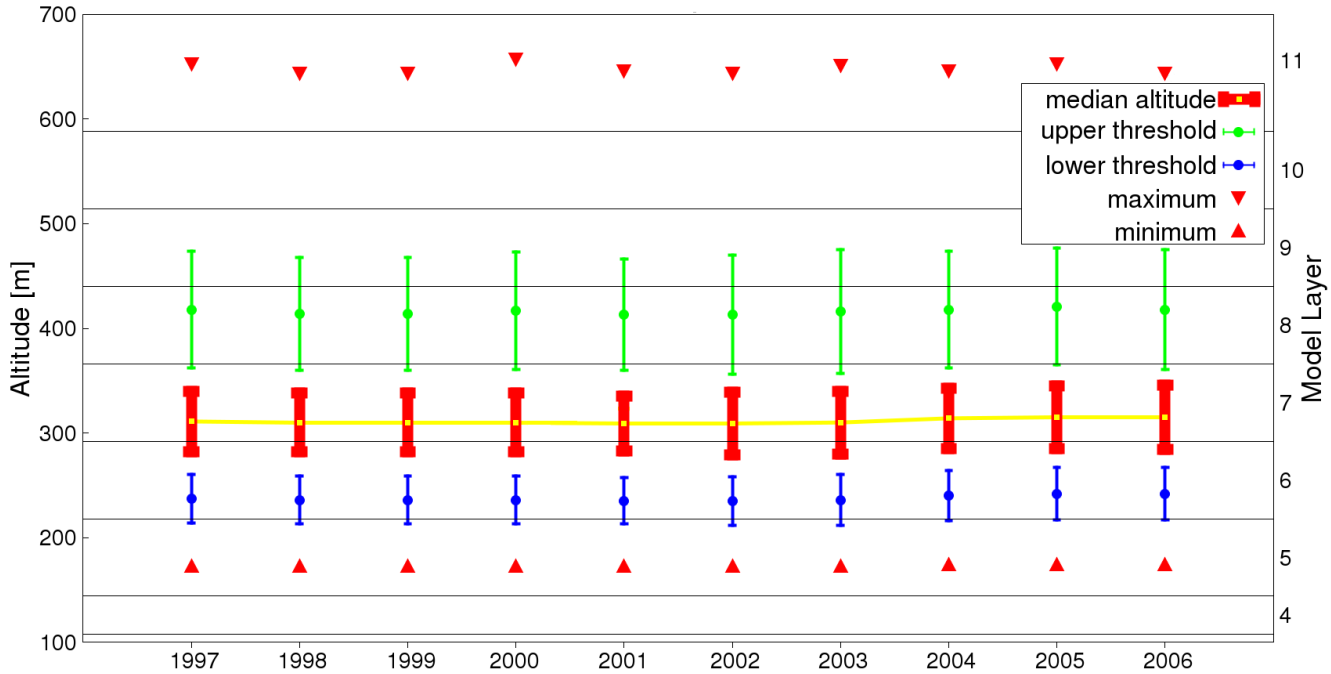

Figure 6: Characterization of emission profiles for ten consecutive years calculated with hourly meteorological fields from the COSMO-CLM climate model. The difference between years is much smaller than the difference between meteorological models. Generally COSMO-CLM leads to a larger spread of the emissions.

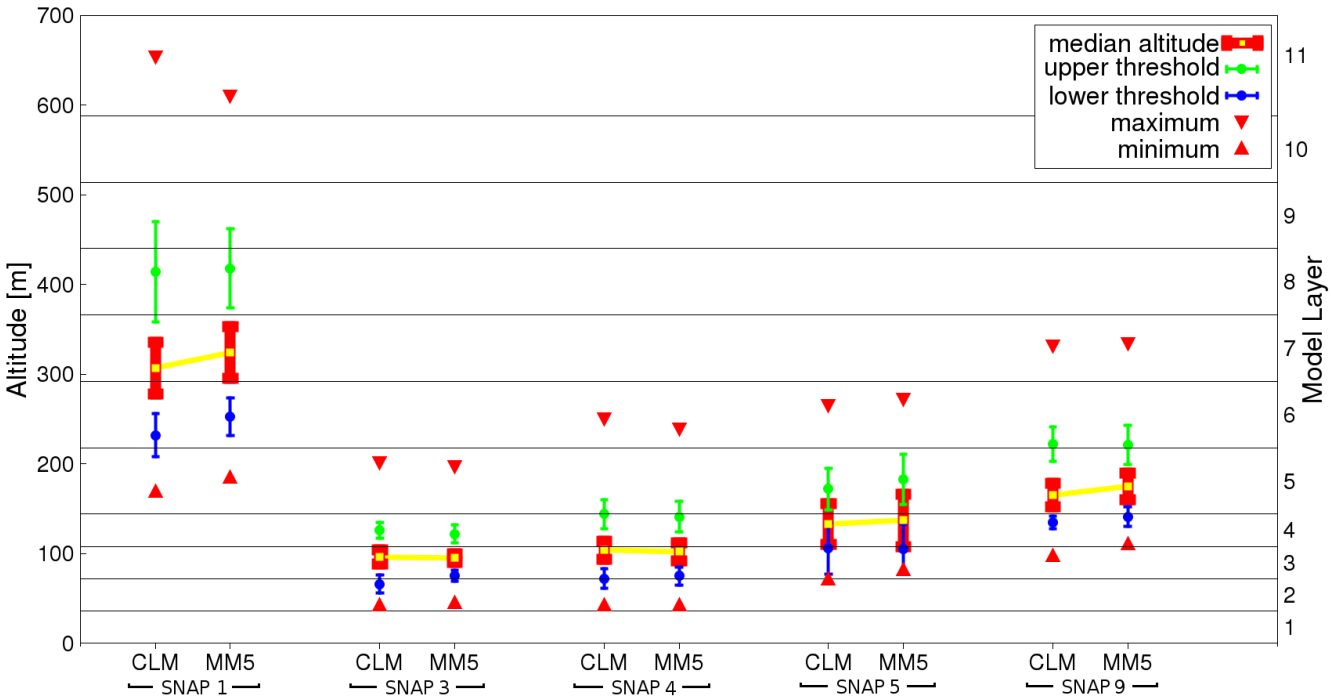

Figure 7: Comparison of emission profiles based on COSMO-CLM and MM5 meteorological fields.

The small effect of the inter-annual meteorological variability on effective emission heights indicates that it is reasonable to use the same set of averaged profiles for different years.

The emission profiles calculated using different meteorological data show the largest differences for SMOKE-EU runs using data from different meteorological models. The comparison of emission profiles calculated with meteorological fields from COSMO-CLM and MM5 lead to differences in the range of 5% to 10% in average median emission altitude and 10% to 20% for the average emission range (Fig. 7). This can be explained by large differences in wind speed. In altitudes above 100m the average wind speeds over the European continent calculated with COSMO-CLM are systematically higher by 1-2 m/s compared to the wind speeds calculated with MM5 (Fig. S13 c). Thus, the MM5 meteorology leads to higher effective emission heights for emissions from the SNAP sectors 1, 5, and 9. For emissions originating from SNAP sectors with median altitudes below 100m (SNAP sectors 3 and 4) the MM5 meteorology leads to slightly lower effective emission heights. Generally, the meteorological fields calculated with COSMO-CLM lead to a larger spread of emissions from high stacks with up to 50% higher standard deviations.

The differences in calculated effective emission heights using data from MM5 nudged to ERA40 using FDDA and COSMO-CLM nudged to NCEP using spectral nudging show the large influence of the meteorological fields. It can not be determined here whether the meteorological model, the reanalysis data used, or the nudging method applied has the larger influence. As figure 6 and 7 indicate, the differences between the effective emission heights calculated with MM5 and COSMO-CLM are much larger than the inter-annual variability over ten years using COSMO-CLM data.

Only minor differences (1-2%) can be observed for runs using different resolutions (Fig. 8). This can be explained by the fact that the vertical emission profiles are national and seasonal averages. It can be expected that this difference is larger when comparing individual sources and hourly values. This supports the view that the emission profiles can be used for a variety of model resolutions and not only the resolution they were calculated with.

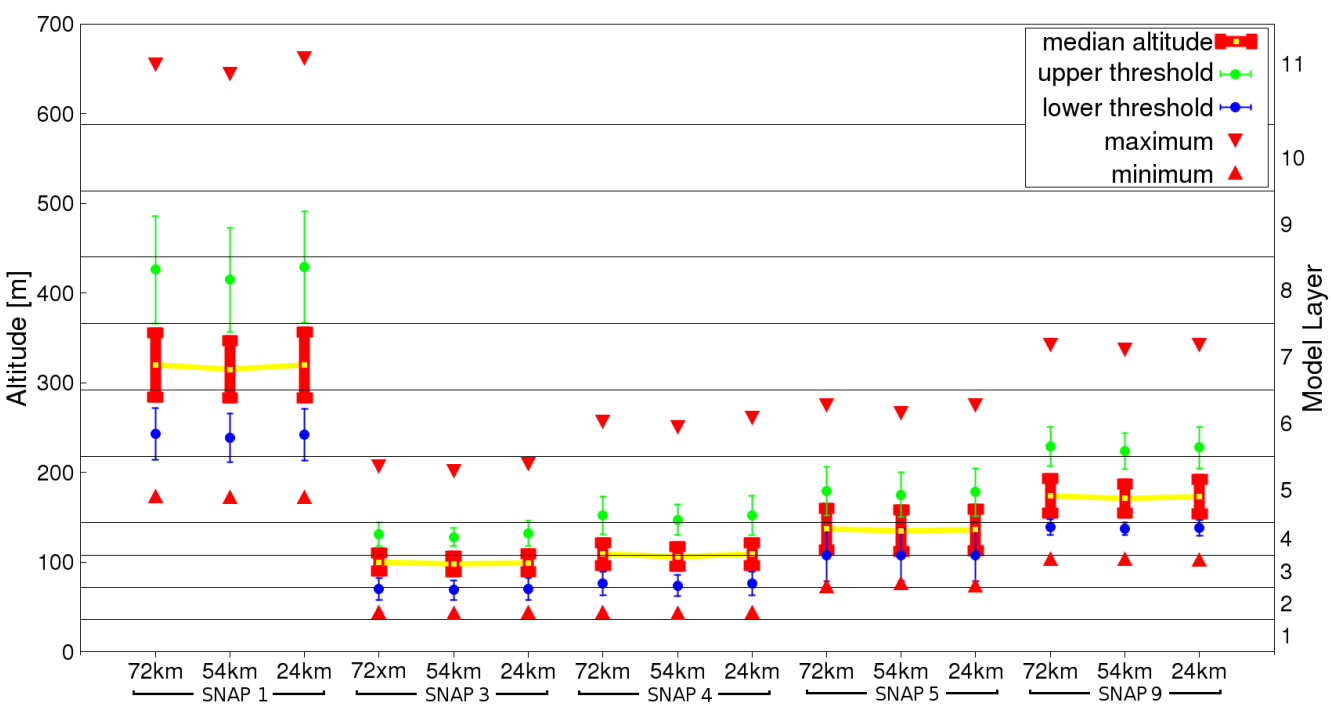

Figure 8: Characterization of emission profiles calculated using different resolutions for the meteorological and the emission model. The model resolutions used are 72x72km², 54x54km², and 24x24km².

Table 3

Comparison of EMEP emission profiles with sectoral averages from this study. The emission profiles from this study were aggregated to the EMEP vertical layers. The profiles from this study take into account emissions from stacks only. For SNAP sectors 4,5, and 9 the assumption has been made that the EMEP emissions in the surface layer are equal to the amount of fugitive emissions. The resulting profiles are shown in the rows marked 'fugitive'. Also see Figure 9 for a more detailed comparison of emission profiles.

SNAP sector		Emission layer [m]					
		0-92	92-184	184-324	324-522	522-781	781-1106
1. Combustion in energy and transformation industries	EMEP			8%	46%	29%	17%
	this study		0.25%	51%	45.3%	3.25%	0.2%
2. Non-industrial combustion plants	EMEP	50%	50%				
	this study	100%					
3. Combustion in manufacturing industy	EMEP		4%	19%	41%	30%	6%
	this study	21.3%	75.4%	3.3%			
4. Production processes	EMEP	90%	10%				
	this study	19%	71%	10%			
	fugitive	***90%***	*7%*	*1%*			
5. Extraction of fossil fuels	EMEP	90%	10%				
	this study	9%	61%	30%			
	fugitive	***90%***	*6%*	*3%*			
9. Waste treatment and disposal	EMEP	10%	15%	40%	35%		
	this study		41%	57%	2%		
	fugitive	***10%***	*37%*	*51%*	*2%*		

3.2 Comparison with existing profiles

The vertical emission profiles calculated in this study were compared with emission profiles from the literature. The widely used emission profiles from EMEP are based on five years of plume rise calculations for industrial plants in Zagreb, Croatia using algorithms referred to as 'standard Briggs' which are not further specified (Vidic, 2002). The wind profiles used for the calculations were obtained from radio soundings. The sectoral emission profiles are based on the plume rise of 8 industrial sources with stack heights of 200m, 150m and 60m.

The emission profiles published by de Meij (2006) are a modified version of the EMEP profiles ($EMEP_{MOD}$). They only distinguish four vertical layers (surface, ~150m, ~250m. high altitude). The main difference is that $EMEP_{MOD}$ includes different profiles for gaseous and particulate species. For comparison with existing vertical profiles, the emission profiles calculated with SMOKE-EU were averaged for five SNAP sectors. Table 3 shows a comparison of the fractions emitted for different SNAP sectors in each layer when using the EMEP profiles compared to the fractions emitted by SMOKE-EU profiles interpolated to the EMEP vertical resolution. SMOKE-EU vertical emission profiles reveal significant differences to the EMEP profiles. Figure 9 depicts a more detailed comparison of emission profiles from this study averaged for five SNAP sectors with profiles used by EMEP. For SNAP sector 1 the median altitude for SMOKE-EU is 300m and there are no emissions higher than 600m, while in the EMEP profiles the median altitude is 500m and emission reach up to 1100m. For SNAP sector 3 the median altitude is 275m in the EMEP profiles and 90m in the sectoral profiles from this study. In general, SMOKE-EU emissions from combustion processes which include power plants (SNAP 1), combustion in manufacturing industries (SNAP 3) and waste incineration (SNAP 9) are allocated to much lower altitudes than in the EMEP profiles. This is most prominent for SNAP3 where the emission ranges do

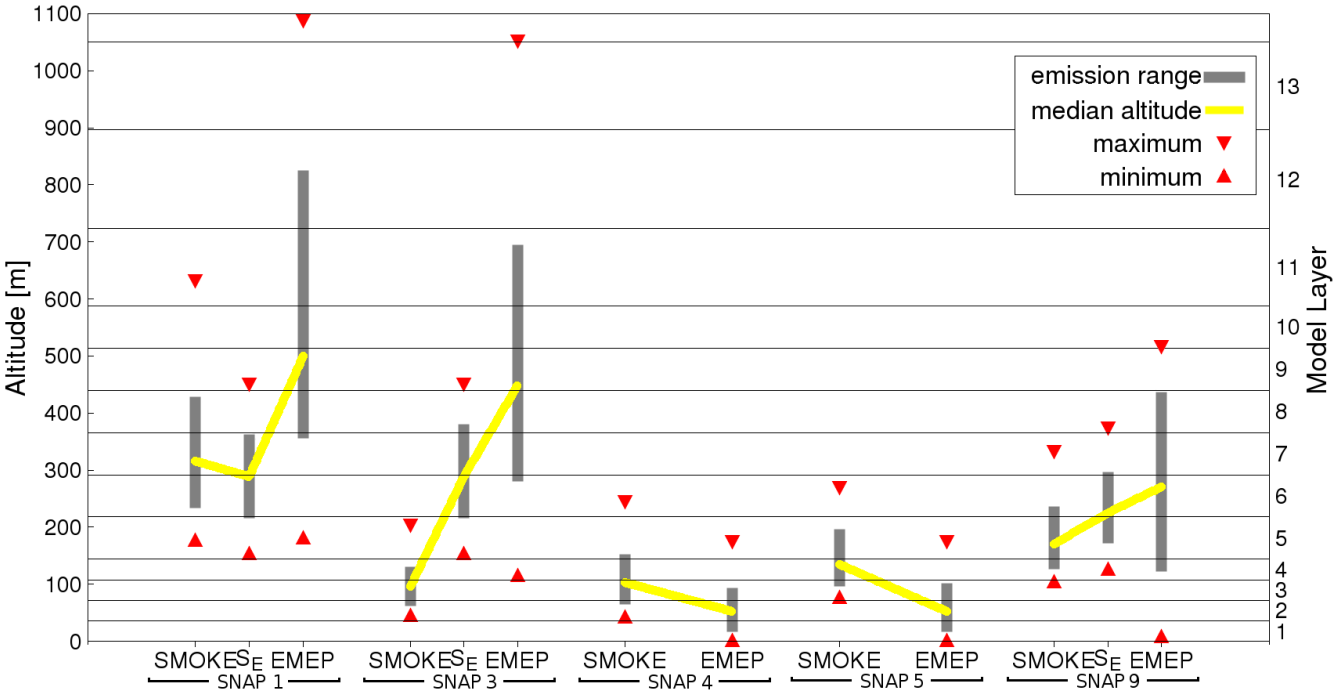

Figure 9: Comparison of emission profiles from this study (SMOKE) averaged over five SNAP sectors (Table 1) with profiles used by EMEP (EMEP). Additionally two SMOKE runs using stack properties from the EMEP report were performed (SE – SMOKE using EMEP stack profiles) (Vidic, 2002).

not overlap at all. Emissions from industrial manufacturing processes (SNAP 4) and extraction of fossil fuels (SNAP5), however, show to be in higher altitudes than in the EMEP profiles where 90% are in the surface layer (<92m). This leads to the fact that although the new vertical profiles on average have higher emissions in much lower altitudes than the EMEP profiles, there are still lower emissions in the near surface layers. This effect may be the result of the higher vertical resolution of SMOKE-EU. With 36m thickness of the lowest 4 layers many low-altitude emissions are still above the surface layer, leading to more transport and chemical reactions before deposition. The emission profiles presented here only take into account emissions from stacks. However, especially the split in diffuse industrial emissions and stack emission from a facility is difficult and deserves further attention. When using the SMOKE-EU profiles it has to be taken into account that, depending on the SNAP sector, a significant part of the emissions can be fugitive emissions. The percentage of fugitive emissions assumed in the EMEP profiles is not known but can be assumed to be between zero and the amount of emissions in the surface layer. The fractions emitted in each layer when assuming that all EMEP emissions in the surface layer are fugitive emissions are introduced in Table 3 in the rows marked 'fugitive'.

To understand the large differences to the EMEP profiles, SMOKE-EU has been used to calculate effective emission heights using the stack characteristics from the EMEP report (Vidic, 2002). The results are depicted in Figure 9 using the abbreviation SE (SMOKE using EMEP profiles). The main differences are higher exit velocities with 13m/s to 18m/s (Vidic, personal communication). The emission-weighted profiles used for this study have an average exit velocity of 6.14 m/s with a standard deviation of 4.34 m/s. Also the stack heights used by EMEP are higher (60-200m instead of 25-120m). Roughly 50% of the difference to the EMEP profiles can be explained by different stack properties. The remaining difference is probably due to the meteorological data from measurements used for the EMEP profiles. Also some *Briggs* algorithms are known to overestimate effective emission heights by up to 30% for neutral temperature stratification (Pregger and Friedrich, 2009). Since the meteorological data as well as the plume rise formulas

used by EMEP are not available this can not be analysed further. The larger vertical spread of the EMEP profiles can be explained by the low vertical resolution of the profiles.

Comparison of SMOKE-EU profiles with the $EMEP_{MOD}$ profiles shows slightly better agreement with profiles from this study (Table 4). For example effective emission heights for SNAP 1 gaseous emissions in $EMEP_{MOD}$ are the same as in the EMEP profiles while SNAP 1 aerosol emissions show better agreement with values from this study. The largest differences are found for sectors SNAP 4 and 9 where 100% of the aerosol emissions are released in the surface layer. The large differences between gaseous and aerosol emissions in the $EMEP_{MOD}$ profiles could not be reproduced by this study, where only minor differences are found.

Table 4

Comparison of modified EMEP profiles ($EMEP_{MOD}$) used by De Meij et al. 2006 with sectoral averages from this study. The emission profiles from this study were aggregated to four layers: 0m-100m, 100m-200m, 200m-300m, above 300m.

SNAP sector		Emission height gas [m]				Emission height aerosol [m]			
		surface	~150m	~250m	high	surface	~150m	~250m	high
SNAP 1	$EMEP_{MOD}$			8%	92%	20%	20%	40%	20%
	this study		0.5%	51%	48.5%			50%	50%
SNAP 2	$EMEP_{MOD}$	50%	50%			100%			
	this study	100%				100%			
SNAP 3	$EMEP_{MOD}$	50%	50%			70%	7.5%	15%	7.5%
	this study	21%	75%	4%		21%	75%	4%	
SNAP 4	$EMEP_{MOD}$	90%	10%			100%			
	this study	19%	71%	10%		18%	72%	10%	
SNAP 5	$EMEP_{MOD}$	90%	10%			20%	20%	40%	20%
	this study	11%	61%	28%		2%	60%	38%	
SNAP 9	$EMEP_{MOD}$	80%	20%			100%			
	this study		41%	57%	2%		42%	57%	1%

3.3 Evaluation of clustered profiles

Using hierarchical cluster analyses the number of aggregated average emission profiles was reduced from 44 976 to 73. This means that many of the spatially and temporally aggregated profiles are not very different. The most significant differences were observed for day and night profiles, where 75% of the profiles refer to different cluster groups (Fig. S2). The differences between day and night are most dominant during summer while in winter time, especially in the northern countries, day and night profiles sometimes do not differ considerably. This can be explained by the small temperature variations in northern European countries during winter. Furthermore, the aggregated profiles show large differences between summer and winter. During winter wind speeds are on average 3 m/s higher (Fig. S13c) and stable atmospheric conditions are much more dominant (Fig. S14) than during summer. Some profiles for spring and autumn are similar to summer or winter profiles. 25% of all spring profiles and 33% of all autumn profiles refer to distinct cluster groups (Fig. S3). The emission profiles for different species regularly fall into separate clusters (Fig. S4). This is most dominant for emissions of VOC from SNAP sector 5 (fugitive emissions from oil production).

The averaged emission profiles have been spatially aggregated in two steps, on the one hand following political regions (countries, groups of countries e.g. north Africa, or parts of countries e.g. Russia) (for details see supplementary A, Lists S1 and S2) and on the other hand according to climate regions (Table 2).

Many countries have one predominant climate region covering more than 95% of the area (Germany, Poland, Denmark, Czech Republic, Ireland, Estonia, Latvia, Lithuania, Belarus, Hungary, Finland, Iceland) (Fig. 3). For these countries the differentiation of climate regions has no impact on the emission profiles. Yet, some countries are split into two or more climate regions. These are mostly riparian states of the Mediterranean Sea (Spain, France, Italy, Croatia, Albania, Greece) which have a Mediterranean climate in the south and a different dominant climate in the north. For these countries differences up to 10% in median emission heights were found for different climate regions. This can be explained by differences in the temperature profiles. Also the coastal areas in the Mediterranean countries, on average, are often characterized by different wind speeds than the rest of the country. Figure 10 depicts seasonal day and night profiles for two climate regions in France as an example. It can be seen that there are large differences between the profiles for winter, summer, and autumn while the spring profiles differ only slightly. Generally the seasonal variation of emission profiles is low in Mediterranean regions which often leads to the application of the same clustered profiles for each season. Some other countries are split into a part with warm temperate climate and one with continental climate (e.g. Norway, Sweden, Romania, Slovakia). The influence of the climate region on the emission profiles in these regions is much smaller than in Mediterranean countries. This is due to the fact that the meteorological differences between these climate regions are not as important for plume rise calculations. To provide an example, figure 11 shows the results for Norway.

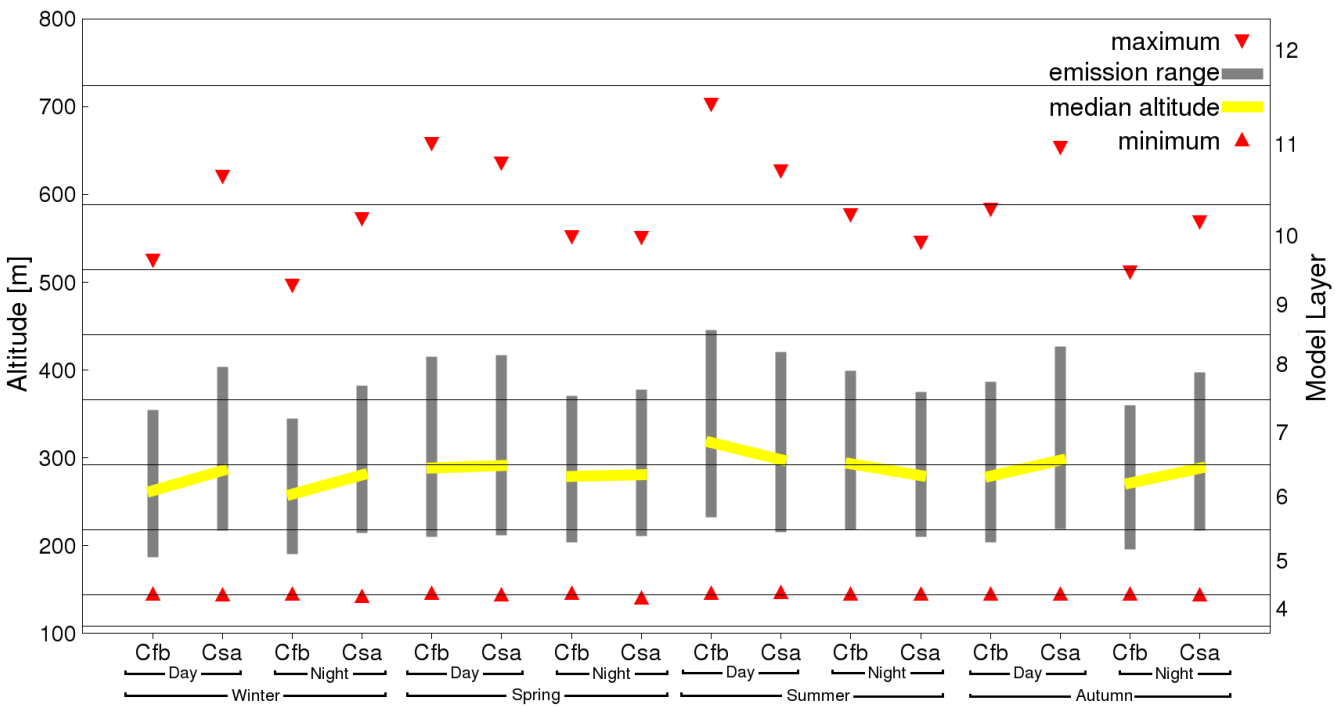

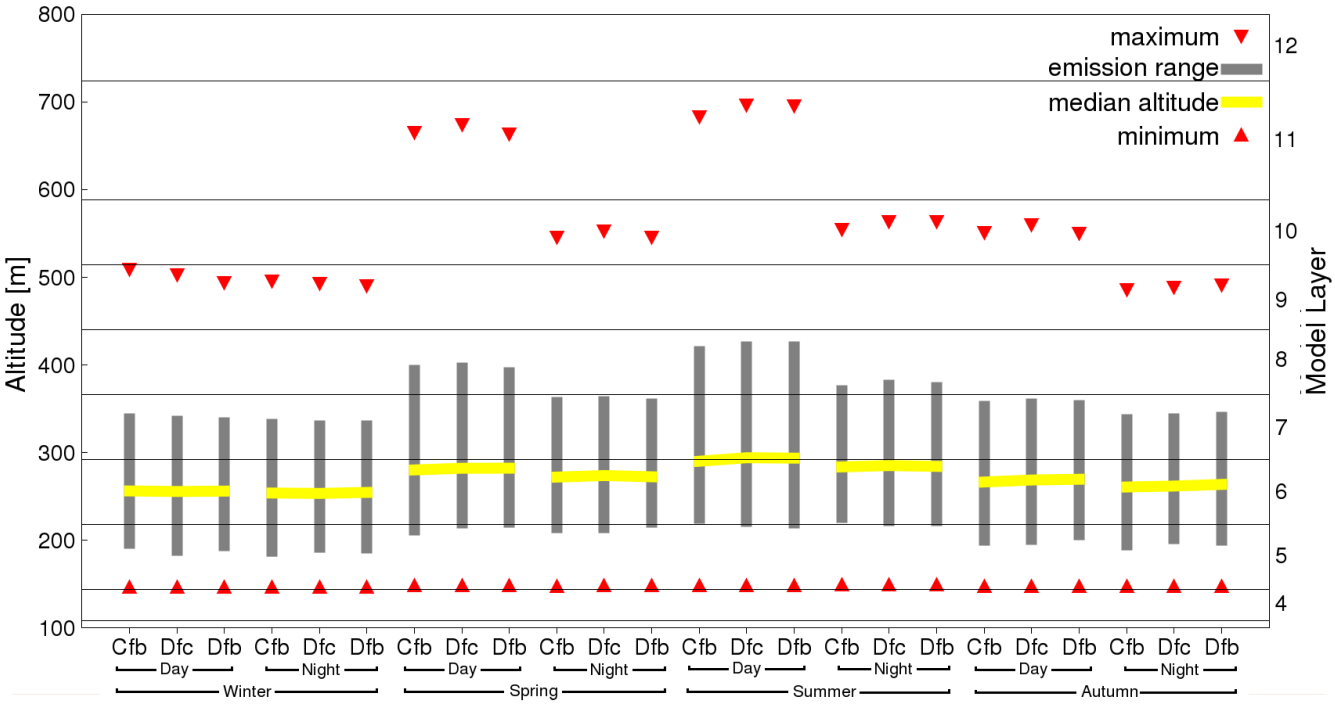

Figure 11: Temporal (4 seasons, day and night) aggregated emission profiles from SNAP sector 1 for different climate regions in Norway. The climate regions are depicted in Figure 3 and explained in Table 2.

3.4 Influenced of emission profiles on calculated surface layer concentrations

To investigate the influence different vertical emission profiles have on surface layer concentrations calculated by CTMs that use emissions as input the Community Multiscale Air Quality (CMAQ) modeling system System was run both with emissions using point source profiles from this study and the EMEP profiles. CMAQ was run on a 54x54 km² domain with 30 vertical layers for January and for July 2000 allowing a spin up time of 12 days in each case. Meteorological fields from the COSMO-CLM model were used as meteorological driver. Boundary conditions were taken from the TM5 model (Krol et al., 2005). Because a full analysis of the CTM results would be beyond the scope of this paper only the most important species emitted by point sources, SO_2 and SO_4^{2-}, were subject of the investigations.

As expected predicted concentrations in the surface layer are higher using the new vertical emission profiles (Fig. 12). In the EMEP run higher concentrations were only found in January in rural regions of Spain, in the south of France and Austria. In January the largest differences between the two runs are observed over the eastern European countries, Spain, and Great Britain. For SO_4^{2-} also large differences are found in the Po valley and around Paris. During July the largest differences in modeled SO_4^{2-} concentrations are found over the Rhine-Ruhr metropolitan area, the Spanish peninsula, and Poland (Fig. S15). Even for grid cells with high concentrations differences of up to 40% for SO_2 and up to 20% for SO_4^{2-} are observed (Fig. S17).

The largest SO_X concentrations in Europe are found between 45°N and 50°N because there the most and biggest industrial plants within Europe are located. In this area the CMAQ run using the new vertical profiles leads to higher SO_2 concentrations up to an altitude of 400m (Fig. S16a-d) while above 500m SO_2 concentrations are higher using the EMEP profiles. This agrees with the fact that the effective emission heights in the EMEP profiles can reach up to 1000m while with the new profiles they were in maximum 600m. Similar results were found for SO_4^{2-} during January (Fig. S16e,f) while in July the EMEP emission profiles lead to slightly higher concentrations above the lowest model layer (36m) (Fig. S16g,h). Generally the influence of the emission profiles on the vertical concentration distribution of particular SO_4^{2-} which is mainly formed by oxidation of SO_2 is smaller than on SO_2 which is directly emitted.

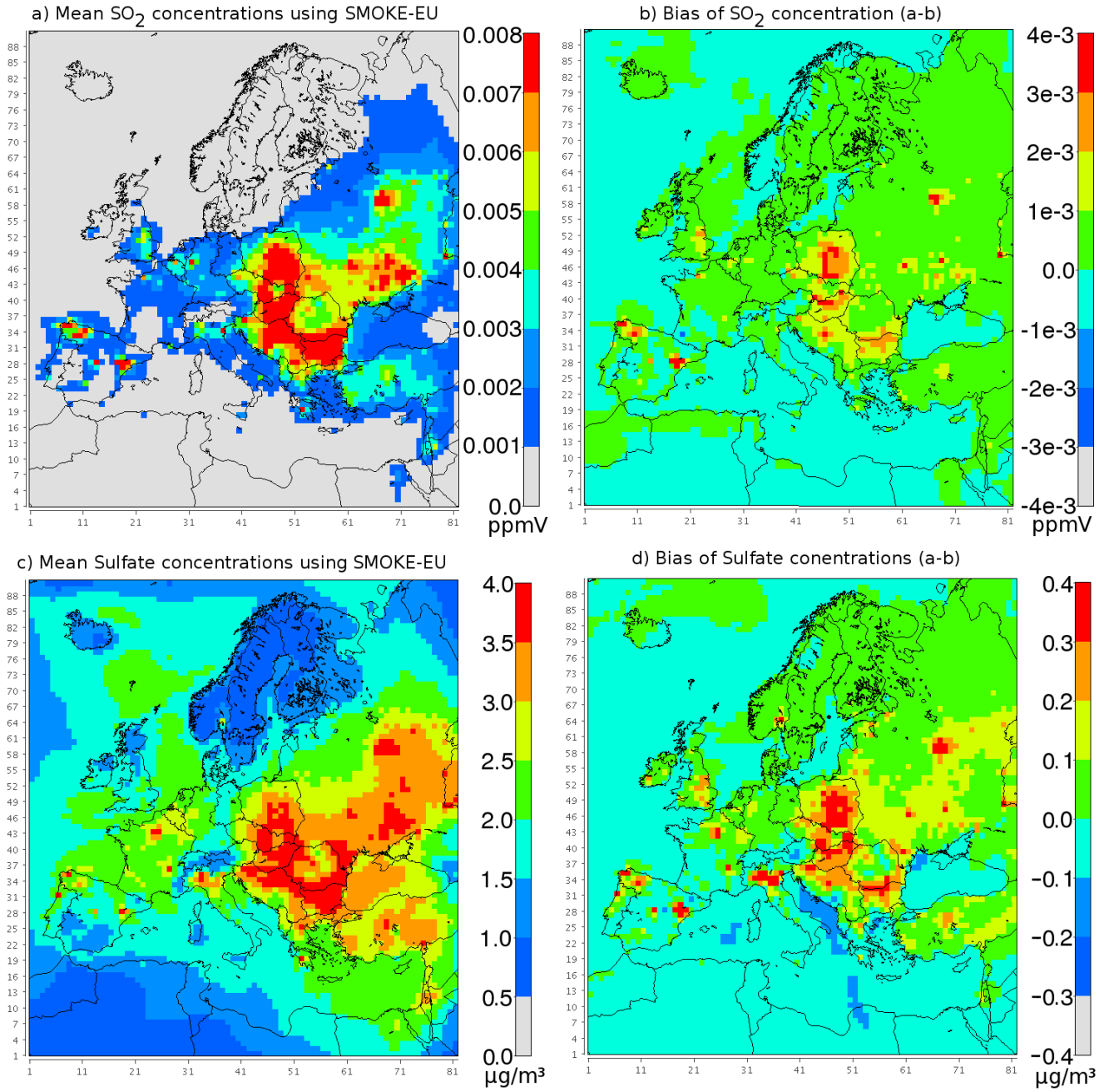

Figure 12: Modeled concentrations of SO2 (a) and SO42- (c) in the lowest model layer (0m-36m) for January 2000 when using the 73 vertical emission profiles from this study. Also depicted is the bias between concentrations modeled with emissions based on the 73 profiles from this study with modeled concentrations based on emissions using EMEP profiles for SO2 (b) and SO42- (d). Positive values indicate that concentrations are higher using the profiles from this study. Results for July can be found in supplementary C.

Additionally the CMAQ run using the 73 profiles from this study was compared to a CMAQ run using the SMOKE-EU emissions with hourly plume rise calculations based on COSMO-CLM meteorological fields for the year 2000. For SO_4^{2-} concentrations in the surface layer the bias between the two CMAQ runs is lower than 2% in January and less than 1% in July (Fig. S18c,d). For SO_2 the run using the 73 profiles from this study leads to 1% to 6% lower concentrations for both months (Fig. S18a,b). The 73

vertical emission profiles have slightly higher effective emission heights than the SMOKE-EU emissions used for comparison because they are based on meteorological fields from COSMO-CLM and MM5, while the plume rise comparison run is based on COSMO-CLM data only. This can explain the fact that the bias is slightly negative for the whole domain. In summary it can be stated that the 73 fixed vertical emission profiles lead to similar surface concentrations as emissions based on hourly plume rise calculations.

4. Conclusions

Vertical emission profiles of point source emissions over Europe have been calculated using average effective emission heights derived from a multitude of plume rise calculations considering different meteorological fields and stack characteristics. The meteorological fields have been created with different models for different years. Different stack characteristics were derived from 34 emission-weighted average stack categories taken from a study by Pregger and Friedrich (2009) and one characterization for coke ovens by Yang et. al (1998). The emission profiles presented here distinguish between 5 source sectors, 48 political regions, 13 climate regions, 4 seasons, day and night, and 6 pollutants. The model ready point source emissions were calculated with emission data from the European Point-source Emission Register (EPER) using the emissions model SMOKE-EU. Emission calculations on a model domain with 54x54 km² grid cell size and 30 vertical layers considering all different cases yielded 44 976 emission profiles from which 73 groups were derived by means of a hierarchical cluster analysis. The 73 clustered profiles as well as a list linking each combination of country, climate region, season, time of day, pollutant emitted and source sector to one of the profiles is published in the supplementary material of this publication.

The influence of different input parameters on the plume rise calculations has been evaluated. The inter-annual variability of the emission profiles as well as the influence of the model resolution were small (1-2%). This indicates that the profiles are largely applicable on regional scales regardless of model resolution and year. The largest uncertainties resulted from the limited availability of source specific data on stack properties followed by the meteorological fields used for plume rise calculations. The stack properties had the largest influence on the effective emission height while the meteorological fields had the largest influence on the vertical spread of the emissions.

The major differences of effective emission heights for SNAP sectors 1,3, and 9 compared to the widely used EMEP profiles can be partially explained by differences in the flue gas exit velocity and stack height used for plume rise calculations. EMEP uses exit velocities estimated from stack height which lie in the range of 13m/s to 18m/s. The emission-weighted profiles used for this study, which are based on real world measurements, have an average exit velocity of 6.14 m/s with a standard deviation of 4.34 m/s (Pregger and Friedrich, 2009). Stack heights used for industrial sources in the EMEP profiles are between 60m and 200m while data from Pregger and Friedrich suggests that the stack heights are between 25m and 120m. For SNAP sectors 4 and 5 EMEP allocates the majority (90%) of the emissions to the surface layer which is 92m thick. In this study 10% to 20% of the emission are emitted below 92m.

Since the inter-annual meteorological variability and the model resolution has only a small influence on effective emission heights and detailed stack profiles for individual sources are not available on a European level the use of fixed vertical emission profiles can substitute plume rise calculations. However, when using fixed emission profiles it is necessary to take into account the annual and daily variability as well as regional differences and not only the source sector and the emitted species. For some countries emission profiles were considerably different depending on climate region. Especially for Mediterranean countries it is recommended to use particular emission profiles for coastal areas. Further improvements of vertical emission profiles can only be achieved by using individual stack data for each industrial plant. Finally, the accuracy of calculated profiles is limited by the meteorological fields. Good agreement between CTM results obtained from runs using the 73 fixed profiles from this study and runs with hourly plume rise calculations proved the applicability of the here presented vertical emission profiles.

Appendix A

SMOKE plume rise formulas as described by Houyoux (1998)

Surface heat flux scale:

$$h^* = \frac{gH_s}{T_g} \qquad \text{(Eq. A1)}$$

Buoyancy flux:

$$F_b = g\frac{T_s - Ta}{T_s}\frac{v_s d_s^2}{4}, if T_s > T_a \qquad \text{(Eq. A2)}$$
$$F_b = 0, \quad if T_s \leq T_a$$

Stability parameter:

$$s = \frac{g}{T_a}\frac{\partial \Theta_v}{\partial z} \qquad \text{(Eq. A3)}$$

Stable-atmosphere plume rise:

$$\Delta h = 2.6\left[\frac{F_b}{us}\right]^{1/3} \qquad \text{(Eq. A4)}$$

Neutral atmospheric stability plume rise:

$$\Delta h = 1.2\left[\frac{F_b}{u\,u_*^2}\right]^{3/5}\left[h_s + 1.3\frac{F_b}{u\,u_*^2}\right]^{3/5} \qquad \text{(Eq. A5)}$$

Unstable-atmosphere plume rise:

$$\Delta h = 30\left[\frac{F_b}{u}\right]^{3/5} \qquad \text{(Eq. A6)}$$

Momentum plume rise:

$$\Delta h_m = 3.0\frac{d_s v_s}{u} \qquad \text{(Eq. A7)}$$

Residual buoyancy flux for
previous layer with neutral atmospheric stability:

$$F_r = \frac{u_l \Delta z_p\, u_*^2}{2.664}\left[\frac{\Delta z_p}{h_s + \frac{2}{3}z_p}\right]^{2/3} \qquad \text{(Eq. A8)}$$

Residual buoyancy flux for
previous layer with stable atmosphere:

$$F_r = \frac{u_l s \Delta z_p^3}{59.319} \qquad \text{(Eq. A9)}$$

Residual buoyancy flux for
previous layer with unstable atmosphere:

$$F_r = u_l\left[\frac{\Delta z_p}{30}\right]^{5/3} \qquad \text{(Eq. A10)}$$

Total plume rise:

$$z_p = z_{(l-1)} + z_p' \qquad \text{(Eq. A11)}$$

Plume top:

$$h_{top} = h_s + 1.5\Delta h \qquad \text{(Eq. A12)}$$

Plume bottom:

$$h_{bot} = h_s + 0.5\Delta h \qquad \text{(Eq. A13)}$$

d_s	stack diameter at stack height [m]
F_b	buoyancy flux [m^4/s^3]
F_r	residual buoyancy flux [m^4/s^3]
g	gravitational acceleration [m^2/s]
H_s	sensible heat flux [mK/s]
Δh	plume rise (to center of plume) equals plume thickness [m]
Δh_m	momentum plume rise (to center of plume) [m]
h^*	stack heat flux scale [m^2/s]
h_{bot}	plume bottom [m]
h_s	stack height [m]
h_{top}	plume top [m]
ρ_z	pressure at altitude z [Pa]
s	stability parameter
T_z	Temperature at altitude z [K]
T_a	ambient temperature at top of the stack (interpolated from layers to h_s) [K]
T_g	surface temperature [K]
T_s	exhaust temperature from the stack [K]
u	wind speed at the top of the stack [m/s]
u_*	surface friction velocity [m/s]
u_l	wind speed in 'current' layer at horizontal location of the stack [m/s]
v_s	stack exhaust velocity [m/s]

z_{l-1} height of the top of the layer below the current layer [m]

Δz_p height of the plume top minus the height of the next lower layer [m]

z_p total plume rise [m]

z_p' distance from the precious layer's top height to the top of the plume [m]

Θ_v virtual potential temperature [K]

Acknowledgements

US EPA is gratefully acknowledged for the use of SMOKE and CMAQ as well as NCAR/Penn State University for the use of MM5. We are thankful to Beate Geyer for providing the COSMO-CLM meteorological fields and to Twan van Noije from KNMI who provided the TM5 concentration fields used as boundary conditions. Also we want to thank Sonja Vidic for help concerning the EMEP profiles as well as Antoon Visschedijk for his useful comments which helped to improve this paper. Finally our thanks go to three anonymous reviewers whose comments helped to improve this paper substantially.

References

Benedictow, A., Fagerli, H., Gauss, M., Jonson, J.E., Nyiri, A., Simpson, D., Tsyro, S., Valdebenito, A., Valiyaveetil, S., Wind, P., Aas, W., Hjelbrekke, A., Marechova, K., Wankmueller, R., Harmens, H., Cooper, D., Norris, D., Schroeder, W., Pesch, R., Holy, M, 2009. Transboundary Acidification, Eutrophication and Ground Level Ozone in Europe in 2007, EMEP Status Report 2009; July 16, 2009, Norwegian Meteorological Institute (NMI), Oslo, Norway, ISSN 1504-6109 (print), ISSN 1504-6192 (on-line).

Bieser, J., Aulinger, A., Matthias, M., Quante, M., Builtjes, P., 2011. SMOKE for Europe – adaptation, modification and evaluation of a comprehensive emission model for Europe. Geosci. Model Dev., 4, 47-68, doi:10.5194/gmd-4-47-2011, available online: www.geosci-model-dev.net/4/47/2011/

Briggs, G. A., 1969. U.S Army Environmental Center Critical Review Series TID-25075, USAEC Technical Information Center, Oak Ridge, TN, USA.

Briggs, G. A., 1971. Some Recent Analyses of Plume Rise Observation, pp. 1029-1032 in Proceedings of the Second International Clean Air Congress, edited by H. M. Englun and W. T. Beery. Academic Press, New York, USA.

Briggs, G. A., 1975. Plume rise predictions, Lectures on Air Pollution and Environmental Impact Analyses, Workshop Proceedings, Sept. 29-Oct. 3, pp. 59-111, Boston, MA, USA.

Briggs, G. A., 1984. Plume rise and buoyancy effects, Atmospheric Sciences and Power Production, D. Randerson, ed., DOE/TIC-27601 (DE84005177), TN, 850 pp., Technical Information Center, U.S. Dept. of Energy, Oak Ridge, USA.

Byun, D.W., and Binowski, F. S., Sensitivity of RADM to Point Source Emissions Processing, Paper 5.4 presented at the 7th Joint Conference on Applications of Air Pollution Meteorology with the Air and Waste Management Association, Jan. 14-18, 1991, New Orleans, LA, Preprints, American Meteorological Soc., pp. 70-73, Boston, MA,, USA.

Byun, D. W., and Ching, J. K. S. 1999. Science Algorithms of the EPA Models-3 Community Multi-scale Air Quality (CMAQ) Modeling System, EPA/600/R-99/030, US EPA National Exposure Research Laboratory, Research Triangle Park, NC, USA.

Byun, D.W. and K. L. Schere., 2006. Review of the Governing Equations, Computational Algorithms, and Other Components of the Models-3 Community Multiscale Air Quality (CMAQ) Modeling System. Applied Mechanics Reviews, 59, Number 2 (March 2006), pp. 51-77.

De Meij, A., Krol, M., Dentener, F., Vignati, E., Cuvelier, C., Thunis, P., 2006. The sensitivity of aerosol in Europe to two different emission inventories and temporal distribution of emissions. Atmos. Chem. Phys. 6, 4287–4309.

Emery, C., Jung, J., Yarwood, G., 2010. Implementation of an alternative plume rise methodology in CAMx, Work Order No. 582-7-84005-FY10-20, ENVIRON International Corporation, 773 San Marin Drive, Suite 2115 Novato, CA 94998, USA.

European Commission, 2000. Decision 2000/479/EC Commission Decision of 17 July 2000 on the Implementation of a European Pollutant Emission Register (EPER) According to Article 15 of Council Directive 96/61/EC Concerning Integrated Pollution Prevention and Control (IPPC).

European Commission, 2006. Regulation (EC) No 166/2006 of the European Parliament and of the Council of 18 January 2006 concerning the establishment of a European Pollutant Release and Transfer Register and amending Council Directives 91/689/EEC and 96/61/EC.

European Environmental Agency, 2007. EMEP/CORINAIR emission inventory guidebook, EEA, 1049 Brussel, Belgium, Technical Report No. 16/2007.

Grell, G.A., Dudhia, J., and Stauffer, D. R., 1995. A Description of the Fifth- Generation Penn State/NCAR Mesoscale Model (MM5), NCAR technical note 398, NCAR, Boulder, Colorado, USA.

Grell, G.A., Peckham, S.E., Schmitz, R., McKeen, S.A., Frost, G., Skamarock, W.C., Eder, B., 2005. Fully coupled online chemistry within the WRF model, Atmos. Environ., 39, 6957-6975.

Houyoux, M.R, 1998. Technical report: plume rise algorithm summary for the Sparse Matrix Operator Modeling System (SMOKE). Prepared for North Carolina Department of Environment and Natural Resources, UNC, Chapel Hill, North Carolina, ENV-98TR004eTR0v1.0.

Kaufmann, L., Rousseeuw, P.J., 1990. Finding Groups in Data: An Introduction to Cluster Analysis, Wiley, New York.

Krol, M., Houweling, S., Bregman, B., Van den Broek, M., Segers, A., Van Velthoven, P., Peters, W., Dentener, F., Bergmaschi, P., 2005. The two-way nested global chemistry-transport zoom model TM5: algorithms and applications, Atmos. Chem. Phys. 5, 417-432, doi:10.5194/acp-5-417-2005.

Matthias, V., Aulinger, A., Quante, M., 2009. Determination of the optimum MM5 configuration for long term CMAQ simulations of aerosol bound pollutants in Europe, Environ. Fluid. Mech., v9, 1, 91-108.

Morris, R.E., Yarwood, G., Emery, C., Wilson, G., 2001. Recent Advances in CAMx Air Quality Modeling. Presented at the A&WMA Annual Meeting and exhibition, Orlando, FL. available online: www.camx.com/publ/pdfs/camx934_AWMA_2001.pdf.

Pozzer, A., Jöckel, P., Van Aardenne, J,. 2009. The influence of the vertical distribution of emissions on tropospheric chemistry. Atmos. Chem. Phys., 9, 9417–9432.

Pregger, T., and Friedrich, R., 2009. Effective pollutant emission heights for atmospheric transport modelling based on real-world information. Environmental Pollution, 157, 2:552–560, doi:10.1016/j.envpol.2008.09.027.

Rockel, B., Will, A., Hense, A., 2008. The Regional Climate Model COSMO-CLM (CCLM) Meteorologische zeitschrift, 17, 347-248.

Rockel, B., Geyer, B., 2008. The performance of the regional climate model CLM in different climate regions, based on the example of precipitation. Meteorologische Zeitschrift Band 17, Heft 4, p. 487-498.

Rubel, F., Kottek, M., 2010. Observed and projected climate shifts 1901-2100 depicted by world maps of the Köppen-Geiger climate classification, Meteorologische Zeitschrift, 19, 135-141. DOI: 10.1127/0941-2948/2010/0430.

Schaap, M., Roemer, M., Sauter, F., Boersen, G., Timmermans, R., Builtjes, P.J.H., Vermeulen, A.T., 2005. LOTOS-EUROS documentation, Available from: http://www.lotos-euros.nl/doc/index.html , access: 1 January 2010.

Stauffer, D.R., Seaman, N.L., 1990. Use of 4-dimensional data assimilation in a limited-area mesoscale model. 1. Experiments with synoptic-scale data. Monthly Weather Rev 118(6):1250-1277.

Turner, D. B., 1985. Proposed Pragmatic Methods for Estimating Plume Rise and Plume Penetration Through Atmospheric Layers. Atmos. Env., 19, 1215-1218.

UNC Carolina Environmental Program, 2005. Sparse Matrix Operator Kernel Emissions (SMOKE) Modeling System, UNC Chapel Hill, North Carolina, USA, 2005.

Vautard R., Beekmann M., Bessagnet B., Menut L., 2007. Chimere Un simulateur numerique de la qualite de l'air, IPSL, Paris, France (in French).

VDI, 1985. Ausbreitung von Luftverunreinigungen in der Atmosphare; Berechnung der Abgasfahnen-uberhohung. (Dispersion of air pollutants in the atmosphere; determination of plume rise) 1985-06 (German/English), Kommission Reinhaltung der Luft (KRdL) im VDI und DIN – Normenausschuss.

Vidic, S., 2002. Frequency distributions of effective plume height, Internal Technical Note, EMEP, 10 September 2002.

Visschedijk, A.J.H., Denier van der Gon, H.A.C., 2005. Gridded European anthropogenic emission data for NOx, SO2, NMVOC, NH3, CO, PM10, PM2.5 and CH4 for the year 2000, TNO, Appeldoorn, Netherlands, TNO-report B&O-A R2005/106 version2.

Visschedijk, A.J.H., Zandveld, P., Denier van der Gon, H.A.C., 2007. A high resolution gridded European emission database for the EU integrated project GEMS, TNO, Apeldoorn, Netherlands, TNO-report 2007-A-R0233/B.

Vogel, B., Vogel, H., Bäumer, D., Bangert, M., Lundgren, K., Rinke, R., Stanelle, T., 2009. The comprehensive model system COSMO-ART – Radiative impact of aerosol on the state of the atmosphere on the regional scale. Atmos. Chem. Phys., 9, 8661-8680, online: www.atmos-chem-phys.net/9/8661/2009.

Wickert, B., 2001. Berechnung anthropogener Emissionen in Deutschland für Ozonsimulationen – Modellentwicklung und Sensitivitatsstudien. Dissertation, Institute of Energy Economics and the Rational Use of Energy (IER), University of Stuttgart. Available from: http://elib.uni-stuttgart.de/opus/volltexte/2001/ 928/ (in German).

Wickert, B., Friedrich, R., Memmesheimer, M., Ebel, A., 2001. Effects of uncertainties in emission modelling on results of ozone simulation. Contribution to the 2nd Joint UN ECE Task Force & EIONET Workshop on Emission Inventories and Projections, 9–11th May 2001, Geneva.

Wolke, R., Knoth, O. Hellmuth, O., Schröder, W., Renner, E., 2004. The parallel model system LM-MUSCAT for chemistry-transport simulations: Coupling scheme, parallelization and application, in: G.R. Joubert, W.E. Nagel, F.J. Peters, and W.V. Walter, Eds., Parallel Computing: Software Technology, Algorithms, Architectures, and Applications, Elsevier, Amsterdam, The Netherlands, 363-370.

Yang, H.H., Lee, W.J., Chen, S.J., Lai, S.O., 1998. PAH emissions from various industrial stacks. Journal of hazardous materials, v60 i2 p159-174.